Published in final edited form as:
NMR Biomed. 2011 November ; 24(9): 1054–1062. doi:10.1002/nbm.1653.

In vivo detection of intermediary metabolic products of [1-^{13}C]ethanol in the brain using ^{13}C magnetic resonance spectroscopy

Yun Xiang and **Jun Shen***
Molecular Imaging Branch, National Institute of Mental Health Intramural Research Program, National Institutes of Health, Bethesda, MD, United States

Abstract

In the present study, in vivo ^{13}C magnetic resonance spectroscopy (MRS) was used to study the labeling of brain metabolites after intravenous administration of [1-^{13}C]ethanol. After [1-^{13}C]ethanol was systemically administrated to the rats, ^{13}C labels were detected in glutamate, glutamine and aspartate in the carboxylic and amide carbon spectral region. ^{13}C-labeled bicarbonate HCO_3^- (161.0 ppm) was also detected. Saturating acetaldehyde C1 at 207.0 ppm was found to have no effect on the ethanol C1 (57.7 ppm) signal intensity after extensive signal averaging, providing direct in vivo evidence that direct metabolism of alcohol by brain tissue is minimal. To compare the labeling of brain metabolites by ethanol with labeling by glucose, in vivo time course data were acquired during intravenous co-infusion of [1-^{13}C]ethanol and [$^{13}C_6$]-D-glucose. In contrast to labeling by [$^{13}C_6$]-D-glucose which produced doublets of carboxylic/amide carbons with a J coupling constant of 51 Hz, the simultaneously detected glutamate and glutamine singlets are labeled by [1-^{13}C]ethanol. Since ^{13}C labels originated from ethanol enter brain after being converted into [1-^{13}C]acetate in liver and the direct metabolism of ethanol by brain tissue is negligible, it is suggested that orally or intragastrically administered ^{13}C-labeled ethanol may be used to study brain metabolism and glutamatergic neurotransmission in studies involving alcohol administration. In vivo ^{13}C MRS of rat brain following intragastric administration of ^{13}C-labeled ethanol is demonstrated.

Keywords

in vivo^{13}C MRS; ethanol; acetate; cerebral metabolism

INTRODUCTION

When ethanol, an amphipathic molecule, enters the body, it distributes itself in total body water at equilibrium, and its extracellular and intracellular concentrations are approximately equal (1). In humans, studies have confirmed that ethanol is predominantly metabolized by alcohol dehydrogenase (ADH), catalase (Cata) and cytochrome P450 2E1 (CYP2E1) in liver (Fig. 1). Via oxidative metabolism, liver is responsible for almost the entire process (approximately 90%) of ethanol elimination (1,2). Acetaldehyde, the first-order or direct metabolite of ethanol, has been shown to be potentially toxic for the brain, a characteristic

*Correspondence to: Jun Shen, PhD, Molecular Imaging Branch, National Institute of Mental Health, Bldg. 10, Rm. 2D51A, 9000 Rockville Pike, Bethesda, MD 20892-1527, Tel.: (301) 451-3408, Fax: (301) 480-2397, shenj@intra.nimh.nih.gov.

Disclosure
This work was supported by the Intramural Research Program of the National Institute of Mental Health, National Institutes of Health (NIMH-NIH). The authors have no conflict of interest to disclose, financial or otherwise.

which is thought to be at least partially responsible for promoting chronic alcohol dependence (3). However, whether or not ethanol can be broken down directly in the brain by the in situ enzyme system remains unknown. To date, it remains unclear which chemicals are involved in the process of chronic alcohol dependence or addiction: ethanol, acetaldehyde, or both ethanol and acetaldehyde.

Many early studies of ethanol metabolism in the brain have shown that ethanol is not broken down directly by brain tissues (2,4,5). Acetaldehyde itself does not seem to be able to penetrate the blood-brain barrier (BBB) (6,7); furthermore, blood levels of acetaldehyde are kept extremely low by the powerful hepatic enzyme systems (6), and even when blood acetaldehyde concentrations are high, acetaldehyde can be converted into acetate by enzymes located on the BBB (e.g. aldehyde dehydrogenase (ALDH)) (8,9). Therefore, it appears that it is ethanol itself in the brain that induces chronic alcoholism. However, many recent studies suggest that ethanol may be metabolized by brain tissues and, furthermore, that the joint activity of acetaldehyde and ethanol in the brain has been proposed to be responsible for promoting chronic alcohol dependence (10–13).

Isotopic techniques are very useful for detecting the metabolism of different kinds of chemicals or energy substrates in the brain. ^{14}C, ^{11}C labeled ethanol was previously used to detect the metabolism of ethanol in the body (2,14,15). However, despite the longer half-time ($T_{1/2}$ = 5,730±40 years), ^{14}C labeled ethanol cannot be widely used to observe ethanol metabolism in the human body because of the harmful radiation effect associated with a large dose of ^{14}C-labeled chemicals. Furthermore, ^{11}C-labeled ethanol cannot be used for continuous detection of ethanol metabolism in the body due to its short half-life ($T_{1/2}$ = 20.38min). Recently, ^{13}C magnetic resonance spectroscopy (MRS), combined with the administration of ^{13}C-labeled substrates, has become a powerful tool for investigating brain metabolism (16–18). This method allows the detection of ^{13}C incorporation from ^{13}C-labeled precursors into various carbon positions of metabolites, such as tricarboxylic acid (TCA) cycle intermediates and amino acids. It allows continuous, nondestructive monitoring of metabolic fluxes under different physiological or pathophysiological conditions.

In vivo ^{13}C MRS combined with the infusion of ^{13}C-labeled substrates can be used to measure or observe the TCA cycle as well as the glutamate-glutamine and γ-amminobutyric acid (GABA)-glutamine cycles between neuronal-glial compartments (19–23). Acetate is a known glia-specific substrate that has been used to study cerebral metabolism, neurotransmission and, in particular, the two-compartment neuronal-glial interactions in both humans and animals (24–27). In the body, ethanol is predominantly metabolized into acetate by various powerful hepatic enzyme systems (1,28). However, acetate in the liver is oxidized at a much lower rate than the oxidation of ethanol itself (28). Acetate from the liver will mainly be broken down by extrahepatic tissues, or other organs (29) such as the brain. Therefore, it may be possible to use ^{13}C-labeled ethanol to study brain metabolism and neurotransmission in experiments involving alcohol administration (30).

Given the uncertainty surrounding whether ethanol is directly metabolized in brain, the present study attempted to analyze the chemical reaction between ethanol and acetaldehyde using intravenous [1-^{13}C]ethanol administration combined with ^{13}C magnetization transfer (CMT) in the rat brain. Previously we have demonstrated CMT can detect specific enzymatic reactions and coupled processes in vivo (31–33). We found no significant conversion of ethanol into acetaldehyde in brain. We simultaneously attempted to observe ethanol and/or its multiple byproducts in the central nervous system (CNS) by using ^{13}C MRS time course study. Subsequently, we acquired in vivo ^{13}C MRS spectra following intravenous co-infusion of [1-^{13}C]ethanol and [$^{13}C_6$]-D-glucose, and compared them with those acquired during intragastric co-administration of [1-^{13}C]ethanol and [$^{13}C_6$]-D-glucose.

We simultaneously measured and distinguished multiple peaks from different isotopomer patterns originated from both ^{13}C-enriched substrates in the chemical shift region of carboxylic/amide carbons. We found that ^{13}C labeling of glutamate and glutamine by [1-^{13}C]ethanol is characteristic of that by the glia-specific substrate [1-^{13}C]acetate, therefore opening the possibility of using ^{13}C-labeled ethanol to study brain metabolism and neurotransmission.

METHOD

MR Hardware

All MRS experiments were performed on a Bruker microimaging spectrometer (Bruker Biospin, Billerica, MA, USA) interfaced to an 11.7 Tesla 89-mm bore vertical magnet (Magnex Scientific, Abingdon, UK). This magnet is equipped with a 57-mm i.d. gradient (Mini 0.5; Bruker Biospin, Billerica, MA, USA) with a maximum gradient strength of 3.0 G/mm and a rise time of 100 μs for in vivo studies of adult rats. The ^{1}H and ^{13}C radio frequency (RF) coils were coplanar and made of single-sided printed circuit board. The inner loop is the ^{13}C coil, with an inner diameter and conductor width of 10.8 and 4.3 mm, respectively. The outer loop is the ^{1}H coil with an inner diameter and conductor width of 23.6 and 5.4 mm, respectively. No noise injection was found in the ^{13}C channel due to proton decoupling. The lower end of the system was an aluminum interface box through which RF cables, ventilation tubes, rectal thermal probe, and catheters were connected. A similar design of the RF probe/animal handling system for proton and Proton-Observed, Carbon-13-Edited spectroscopy experiments of rat brain using the vertical 89-mm bore magnet was previously described (34,35). The loaded isolation between ^{1}H and ^{13}C coils (S21), which have a large frequency separation of 375 MHz, is −30.6 dB at 125 MHz and −31.2 dB at 500 MHz, respectively, and the standard Bruker filters were used. A broadband low-pass filter was used in the ^{13}C channel whose insertion loss at 125 MHz was less than 0.5 dB. Its rejection at 500 MHz was greater than 80 dB. In the proton channel, a broadband high-pass filter was used with an insertion loss at 500 MHz less than 0.5 dB and rejection at 125 MHz greater than 60 dB. The integrated RF coils/head-holder system is capable of rat head fixation (with ear pins and a bite bar), body support and RF shielding. The pulse-acquire sequence (18) and that of saturation transfer (31) were applied in the study. ^{1}H decoupled ^{13}C MRS experiments were performed to measure the ^{13}C signals in the animal brain. Anatomical images were acquired using the three-slice (coronal, horizontal, and sagittal) scout rapid acquisition with relaxation enhancement (RARE) imaging method (field of view = 2.5 × 2.5 cm^2, slice thickness = 1 mm, TR/TE = 200/15 ms, rare factor = 8, data matrix = 128×128).

In vivo MRS procedures

After experimental animals were put into the scanner, RARE magnetic resonance imaging (MRI) images were acquired to ensure the animal brain and the RF coils were in the proper position. The gradient isocenter of the RF probe/animal handling system in a Mini 0.5 gradient was about 0–1 mm posterior to bregma. The rat brain was shimmed as described previously using the FASTMAP/FLATNESS method (36).

In vivo ^{13}C saturation transfer experiments were performed as previously described (31–33). The saturation pulse was placed at 207.0 ppm, the resonant frequency of carbonyl carbon of the keto form of acetaldehyde (37–40). The chemical shift of the carbonyl carbon of acetaldehyde was measured in phantom at neutral pH.

Broadband ^{1}H-^{13}C nuclear Overhauser enhancement (NOE) was generated using a train of nonselective hard pulse with a nominal flip angle of 180° space 100ms apart. The decoupler

frequency was placed at 3.6 ppm, the resonance frequency of ethanol H2. ^{13}C continuous-wave (CW) RF saturation of the carbonyl carbon (C1) of acetaldehyde at 207.0 ppm was performed with a nominal RF saturation field (B_{1sat}) of 1.8×10^{-2} Gauss. When the control spectra were acquired, the saturating pulse was placed at an equal spectral distance from ethanol C1 but on the opposite side of acetaldehyde C1. To minimize motion artifacts and interference from slowly varying ethanol signal intensity, the saturation and control spectra were interleaved. A 1-ms adiabatic half passage (AHP) pulse was used for 90° excitation. The ^{13}C carrier frequency was centered near ethanol C1 at 57.7 ppm. WALTZ-4 with a 400 μs nominal 90° rectangular pulse was used for ^{1}H decoupling. A natural-abundance baseline spectrum was also acquired before infusion. No significant overlapping resonances were found at the ethanol C1 resonance.

Because carbon in the carboxylic/amide carbon is only coupled to protons via very weak long-range ^{1}H-^{13}C scalar couplings, ^{13}C-labeled chemicals appearing in this chemical shift region can be effectively decoupled at a very low RF power (41, 42). As a result, decoupling of large one-bond ^{1}H-^{13}C scalar couplings can be avoided by using [1-^{13}C]ethanol because the resonances of its intermediary metabolic products including [1-^{13}C]acetaldehyde (AcHC1, 207.0 ppm), [1-^{13}C]acetate (182.6 ppm), [5-^{13}C]glutamate (GluC5, 182.0 ppm), [5-^{13}C]glutamine (GlnC5, 178.5 ppm), [1-^{13}C] γ-amminobutyric acid (GABAC1, 182.3 ppm), [4-^{13}C]aspartate (AspC4, 178.3 ppm), [1-^{13}C]aspartate (AspC1, 175.0 ppm) appear in the carboxylic/amide spectral region. Furthermore, another advantage of this strategy is the lack of contamination from subcutaneous lipids, because there are no overlapping fat signals in the vicinity of the GluC5 and GlnC5 peaks. For direct detection of ^{13}C labeling of brain metabolites no RF saturation pulses were applied.

Experimental animals

All experimental animals were studied according to procedures approved by the National Institute of Mental Health (NIMH) Intramural Research Program Animal Care and Use Committee, National Institutes of Health (NIH). During the experimental process, all efforts were made to minimize animal suffering, to reduce the number of animals used, and to use alternatives to in vivo techniques, if available. Animals (adult Sprague-Dawley rats, Taconic Laboratories, Germantown, NY, USA) were kept under conditions of constant temperature (21 °C) and humidity (50%), with a 12-hour light/dark cycle and free access to food and water. ^{13}C-enriched [1-^{13}C]ethanol and [$^{13}C_6$]-D-glucose were purchased from Cambridge Isotope Laboratories, Inc (Andover, MA, USA). The enrichment of both ^{13}C-labeled chemicals was 99%. The animals (body weight = 178–255 g) were evenly divided into four groups. Five non-fasting animals (Group A) were given intravenous infusion of [1-^{13}C]ethanol [33% (*vol/vol*)] at a dose of 5 g/kg (body weight (BW)), including an initial bolus of 2 g/kg BW in the first 10 minutes followed by the rest of the chemical for the remaining 270 minutes (3 g/kg BW). Animals in Group B (non-fasting, n = 5) received intravenous infusion of [1-^{13}C]ethanol [33% (*vol/vol*)] at a dose of 4 g/kg BW including a 10 minute initial bolus of 2 g/kg BW followed by the rest of the chemical (2 g/kg BW) for the remaining 170 minutes. Animals in Group C (n = 6) were fasted overnight and received intravenous co-infusion of [1-^{13}C]ethanol [33% (*vol/vol*)] and [$^{13}C_6$]-D-glucose (0.75 M). The [1-^{13}C]ethanol infusion protocol consisted of an initial bolus of 2 g/kg BW for the first 10 minutes followed by infusion of 4 g/kg BW over a maximum period of 350 minutes; the [$^{13}C_6$]-D-glucose infusion protocol consisted of an initial bolus of 75.5 mg/min/kg BW for the first 10 minutes followed by a maximum of 350 minute continuous infusion at 28.5 mg/min/kg BW. Group D animals (n = 3, fasted for 24 hours) were used to acquire in vivo ^{13}C MRS spectra after intragastric co-administration of both [1-^{13}C] ethanol [33% (*vol/vol*)] and [$^{13}C_6$]-D-glucose (0.75 M).

On the day of in vivo ^{13}C MRS study, the animals were orally intubated and mechanically ventilated (SAR-830/AP, CWE, Inc., Ardmore, PA, USA) with a mixture of 70% N_2O, 30% O_2, and 1.5% isoflurane. One artery was cannulated for periodic sampling of arterial blood in order to monitor blood gases (*p*O2, *p*CO2), pH, and blood glucose concentrations using a blood analyzer (Bayer Rapidlab 860, East Walpole, MA, USA), as well as to monitor and regulate arterial blood pressure levels. For Groups A and B animals, one femoral vein was cannulated for infusion of ^{13}C-labeled ethanol; for Groups C and D animals, bilateral femoral veins were cannulated, one for intravenous infusion of [1-^{13}C]ethanol, the other for intravenous infusion of [$^{13}C_6$]-D-glucose. For the rats administered with [$^{13}C_6$]-D-glucose (groups C and D), total plasma glucose levels were maintained at 12.0~16.0 mM during in vivo ^{13}C MRS data acquisition. Throughout the experiment, normal physiological conditions were maintained according to results obtained from the blood analyzer (pH ~7.4, pCO_2 ~35 mmHg and pO_2 > 100 mmHg), respiration monitor (SurgicalVet, SIMS BCI, Inc. Wisconsin, USA), and by real-time regulation of ventilation. Blood pressure, heart rate, and respiration changes were also monitored simultaneously (BIOPAC System, Inc. GenuineIntel, Goleta, CA). An external pump for heat exchange by circulating warm water (BayVoltex, Modesto, CA, USA) was used to maintain body temperature at 37.8 ± 0.5 °C.

RESULTS

^{13}C labeling of brain metabolites following intravenous infusion of [1-^{13}C]ethanol

Figure 2 shows in vivo ^{13}C MRS spectra acquired from one Group A animal after intravenous infusion of [1-^{13}C]ethanol. The results showed that ^{13}C labels carried by infused [1-^{13}C]ethanol were incorporated into carbonyl carbons of multiple metabolites including GluC5 (182.0 ppm), GlnC5 (178.5 ppm), and GluC1 (175.4 ppm). The time domain data were zero-filled to 16 K. Exponential line broadening (lb = 10) was applied before Fourier transform. The ^{13}C-labeled bicarbonate HCO_3- (161.0 ppm) was also detected. Although ethanol itself can be easily detected as a singlet at 57.7 ppm (not shown in Fig. 2), its direct metabolite AcHC1 (207.0 ppm) was not observed. Similar results were obtained for all Group A animals. The chemical shift position of AcHC1 (207.0 ppm) was marked in Fig. 2.

^{13}C saturation transfer

Figure 3(A) shows the results of ^{13}C saturation transfer experiments performed on one Group B animal targeting the [1-^{13}C]ethanol↔[1-^{13}C]acetaldehyde reaction. The difference spectrum (bottom trace) represents signal averaging for 180 min. The difference spectrum (bottom trace) was obtained by subtracting the subspectrum with the saturation of AcHC1 at 207.0 ppm (middle trace) from the control spectrum with the saturation pulse placed at −149.3 ppm (top trace). The results indicate that no significant saturation transfer effect was found for the [1-^{13}C]ethanol↔[1-^{13}C]acetaldehyde reaction in brain. We also added up the results from all Group B animals (n = 5) in Figure 3(B) and no signal above the noise level was detected in the summed difference spectrum. The noise level in Fig. 3B was measured by first integrating the ethanol C1 signal in the control spectrum. Then the same integration interval length was used to divide the difference spectrum into equal segments and to integrate the noise in each segment. The concentration of ethanol was estimated to be 15.4 mM based on separate proton MRS measurements using N-acetylaspartate (NAA) as a concentration reference standard ([NAA] = 10.8 mM, 27). In the proton MRS experiments the infusion protocol used unlabeled ethanol. The noise level (σ) of the difference spectrum was found to be 0.089 mM. Since the detection threshold for 95% confidence interval is 1.65σ, the detection limit using our procedure is 1.65 × 0.089 = 0.15 mM for ethanol C1, which corresponds to a ^{13}C saturation transfer pseudo first order rate constant in the range of 3.2×10^{-3} sec^{-1} ~ 9.7×10^{-3} sec^{-1} (for T_1 = 3~1 sec). That is, the detection threshold of our method for the pseudo first order rate constant of the ethanol acetaldehyde exchange

reaction in rat brain is ca. 0.003~0.01 sec^{-1}. In contrast to the brain, when rat liver homogenate was measured using the same ^{13}C saturation transfer MRS protocol, a prominent drop in the ethanol C1 signal was observed upon irradiating the AcHC1 resonance at 207.0 ppm. The amplitude of the difference ethanol C1 signal was determined to be 72.5% of that in the control spectrum (data not shown), indicating a very fast exchange between acetaldehyde and ethanol in liver.

Simultaneous intravenous administration of [1-^{13}C]ethanol and [$^{13}C_6$]-D-glucose

Figure 4(a) shows the *in vivo* proton decoupled ^{13}C MRS time course spectra of rat brain in the carboxylic/amide carbon spectral region acquired from one animal in Group C during co-infusion of [1-^{13}C]ethanol and [$^{13}C_6$]-D-glucose. The time domain data were zero-filled to 16K. The resolution enhancing Lorentz-Gauss transformation (lb = −5, gb (Gaussian broadening factor) = 0.1) was applied before Fourier transform. ^{13}C labeling of multiple metabolites was detected in the carboxylic/amide region, including GluC5 (182.0 ppm), GluC1 (175.4 ppm), GlnC5 (178.5 ppm), GlnC1 (174.9 ppm), Asp C4 (178.3 ppm) and [1-^{13}C]lactate (183.3 ppm). Each spectrum corresponds to 20-minute signal averaging. The singlets from [1-^{13}C]ethanol (57.7 ppm) and ^{13}C-labeled HCO_3^- (161.00 ppm) were also observed but are not shown here. Figure 4(b) shows the spectrum from one animal accumulated over the 120–360 minute interval after the initiation of co-infusion of [1-^{13}C]ethanol and [$^{13}C_6$]-D-glucose. In separate control experiments using unlabeled ethanol and [$^{13}C_6$]-D-glucose no GluC5 singlets were detected (data not shown). This is expected because the glutamate $^{13}C4$-$^{13}C5$ moiety always comes from [1,2-$^{13}C_2$]acetylCoA regardless of the number of turns of the TCA cycle. Therefore, glutamate C5 singlet cannot be formed as long as [1,2-$^{13}C_2$]acetylCoA is the only labeled input to the TCA cycle. By inference, glutamine C5 and aspartate C4 singlets cannot be formed either under this condition.

Therefore, co-infusion of differently labeled substrates and the detection of signals in the carboxylic/amide ^{13}C spectral region allow clear separation of contribution to glutamate, glutamine and aspartate from the different substrates. As shown in Fig. 4, glutamate C5 originated from [$^{13}C_6$]-D-glucose appears as a doublet with a J coupling constant of 51 Hz while glutamate C5 originated from [1-^{13}C]ethanol appears as a singlet. The large homonuclear ^{13}C-^{13}C J coupling between an aliphatic carbon and a carboxylic or an amide carbon and the lack of interference from other one-bond couplings allow a clear separation of signals originated from singly and doubly labeled substrates. At 11.7 Tesla, the chemical shift separation between glutamine C5 and aspartate C4 is coincidentally one half of the one-bond J coupling between an aliphatic carbon and a carboxylic or amide carbon. As a result, a pseudo quartet was detected in the 178–179 ppm region, allowing easy detection of contributions to glutamine C5 and aspartate C4 from different substrates. Similarly, glutamate C1 originated from [$^{13}C_6$]-D-glucose and singly labeled [1-^{13}C]ethanol were also detected because glutamate C1 is widely separated from glutamine C1, aspartate C1 and NAA C5. Quantitative analysis revealed the expected brain's preference for glucose as the respiration fuel. At 220 min after the initiation of co-infusion (all group C and D rats were infused for a minimum of 230 minutes), $[GluC5]_{Glucose}/[GluC5]_{Ethanol}$, $[GlnC5]_{Glucose}/[GlnC5]_{Ethanol}$ and $[GluC5 + GlnC5 + AspC4]_{Glucose}/[GluC5 + GlnC5 + AspC4]_{Ethanol}$ ratios from Group C animals were found to be (3.29 ± 0.12, 2.65 ± 0.17, 3.36 ± 0.15):1.

Intragastric administration of ^{13}C labels

Figure 5(a) shows the *in vivo* proton decoupled ^{13}C MRS time course spectra acquired from one Group D rat during intragastric co-administration of [1-^{13}]ethanol and [$^{13}C_6$]-D-glucose. Figure 5(b) shows the accumulated ^{13}C MRS spectrum acquired during the 140~360 minute interval after the start of intragastric co-administration of [1-^{13}]ethanol and [$^{13}C_6$]-D-

glucose. Data processing was the same as previously described for the co-infusion experiments (lb = −5, gb = 0.1). At 220 min after the initiation of co-infusion, $[GluC5]_{Glucose}/[GluC5]_{Ethanol}$, $[GlnC5]_{Glucose}/[GlnC5]_{Ethanol}$ and $[GluC5 + GlnC5 + AspC4]_{Glucose}/[GluC5 + GlnC5 + AspC4]_{Ethanol}$ ratios from Group C animals were found to be (4.04 ± 0.36, 0.92 ± 0.13, 2.83 ± 0.34):1. Compared with Group C, the Group D data showed a much slower rate of glucose transport into the brain as expected from the additional delay by the stomach (43). In contrast, ethanol is freely diffusible in the body and therefore not affected by intragastric administration. As a result, the doublet signals originated from intragastrically administered [$^{13}C_6$]-D-glucose are lower in (Fig. 5(b) than the corresponding doublet signals in Fig. 4(b). The largest difference between intravenous and intragastric administration is seen in GlnC5. In Fig. 5(b), singly labeled GlnC5 is rapidly generated in astroglia by ^{13}C labels originated from [1-^{13}C]ethanol. At the same time, the synthesis of doubly labeled GlnC5 is delayed by both the gastric barrier to glucose and the glutamate-glutamine cycle. By the same mechanism, the GluC1 signal of Group C rats originated from [$^{13}C_6$]-D-glucose is much higher than the GluC1 signal of Group D rats originated from [$^{13}C_6$]-D-glucose.

DISCUSSION

The metabolism of ethanol and its intermediary metabolic products in the brain

Previously ^{14}C, ^{11}C-labeled ethanol combined with the techniques of radioactivity test and positron emission tomography (PET) were used to measure the metabolism of ethanol in the body (2,14,15). In one study where ^{14}C-labeled ethanol was used to observe ethanol metabolism in monkeys (44), Mushahwar and colleagues found that some of the glutamate and glutammine in the brain tissue was originated from the ^{14}C-labeled ethanol (14). Because they did not find ^{14}C-labeled acetaldehyde or acetate, their results cannot be taken as evidence that ethanol is broken down directly in the brain. Using results obtained from isolated, perfused rat brain, Mukherji and colleagues concluded that ethanol itself cannot be metabolized by brain directly, although they simultaneously found that acetaldehyde can be broken down by the brain (2). The current study used ^{13}C MRS, combined with the administration of ^{13}C-labeled substrates to study the labeling of brain metabolites by [1-^{13}C]ethanol. We found that ^{13}C labels from [1-^{13}C]ethanol are readily incorporated into glutamate, glutamine and aspartate in brain, suggesting that ethanol and/or its metabolites (e.g., acetaldehyde, acetate) are metabolized by brain tissues (see Fig 2). However, neither AcHC1 (207.0 ppm) nor [1-^{13}C]acetate (182.6 ppm) metabolized from [1-^{13}C]ethanol were detected in the brain ^{13}C MRS spectra. Recent studies of ethanol metabolism reported that the concentration of ethanol and acetaldehyde could reach 40 mM and 250 μM by using an aldehyde dehydrogenase inhibitor (45). Earlier studies have also found that, under normal physiological conditions without using enzyme inhibitors, acetaldehyde levels were only 6.720 μM and 18.165 μM (or: 6.4 nM/g and 17.3 nM/g) for C57 and DBA mice, respectively (46), which were well beyond the detection threshold of in vivo ^{13}C MRS.

Enzymatic activity for acetaldehyde production in the brain

To further explore ethanol metabolism in the CNS, the present study used intravenous [1-^{13}C]ethanol administration combined with ^{13}C saturation transfer to detect the conversion of ethanol to acetaldehyde in the rat brain.

Because fasting reduces ethanol metabolism (47–49), the saturation transfer experiment conducted here did not use animals that had fasted before ^{13}C MRS data acquisition. Results from the saturation transfer showed that when the pulse was set on 207.0 ppm (the resonant frequency of acetaldehyde C1), no significant difference in [1-^{13}C]ethanol signal (57.7 ppm) between the saturation and control spectra was observed (Fig. 3). Because the in vivo ^{13}C

saturation (or inversion) transfer effect of enzyme-catalyzed reactions can be used to measure enzyme-specific reactions in vivo (31–33,50), the negative saturation transfer results obtained here are consistent with previous studies that found minimal ADH, CYP2E1 and catalase activities in brain tissue. In comparison, a large ^{13}C saturation transfer effect caused by the exchange between ethanol and acetaldehyde is easily observable using rat liver homogenate (data not shown).

The results of the present study echo previous work noting that powerful enzyme systems exist for metabolizing ethanol in extracerebral tissues, especially the liver, which is the biggest digestive gland in the body. When entering the body, ethanol is predominantly metabolized into free acetate in the liver, and subsequently enters the bloodstream (1,28,47–49). Thus, after the administration of ethanol, the main role of the brain is simply to use the ethanol product acetate originated from extracerebral tissues. This conclusion is further corroborated by separation proton MRS measurements performed during the course of infusing unlabeled ethanol. Using the same infusion protocol as that used for Group B rats, no change in the lactate signal at 1.32 ppm in the proton time course spectra was found (data not shown). If cerebral ethanol metabolism were significant, the increased NADH/NAD ratio would have caused an elevation of the cerebral lactate signal. The results shown in Figs. 4 and 5 therefore open the possibility that intravenous or oral administration of ethanol could be used to study brain metabolism.

Co-administration of [1-^{13}C]ethanol and [$^{13}C_6$]-D-glucose for the study of cerebral metabolism

Co-administration of [1-^{13}C]ethanol and [$^{13}C_6$]-D-glucose allows simultaneous detection of the labeling kinetics of brain metabolites by singly labeled [1-^{13}C]ethanol and uniformly labeled glucose. Similar to a previous study using infusion of [$^{13}C_6$]-D-glucose (without ethanol) and detection of ^{13}C label incorporation into the alkyl C4 carbons of glutamate and glutamine (35), the results in Figs 4(b) and 5(b) show a temporal lag in the incorporation of ^{13}C labels from [$^{13}C_6$]-D-glucose into the glutamine C5 carbon as compared to the incorporation of ^{13}C labels into glutamate C5 carbons. This is consistent with the recently validated glutamate-glutamine cycle between neurons and astroglia with ^{13}C-labeled neuronal glutamate as the main metabolic precursor for ^{13}C-labeled astroglial glutamine when ^{13}C-labeled glucose is administered. The precursor-product relationship between ^{13}C-labeled neuronal glutamate and ^{13}C-labeled astroglial glutamine is reversed when ^{13}C-labeled acetate is used for introduction of extragenous ^{13}C labels. This is because acetate is predominantly metabolized in the glial cells. Recently, ^{13}C labeled acetate and glucose have been used to study cerebral metabolism, particularly with regards to the relationship between neurons and the glial cells (20,24,51). This reversed precursor-product relationship between ^{13}C-labeled neuronal glutamate and ^{13}C-labeled astroglial glutamine is shown by the results given in Figs. 4 & 5 with co-administration of [1-^{13}C]ethanol and [$^{13}C_6$]-D-glucose. In particular, in Figs 4(b) and 5(b), there is a clear preference by glutamine for ^{13}C labels originated from the singly labeled [1-^{13}C]ethanol.

Accumulating evidence indicated that co-infusion of specific ^{13}C-enriched glucose and acetate could be used to measure both neuronal and glial metabolism in the brain using ^{1}H-decoupled ^{13}C MRS (22). This approach was based on the findings that ^{13}C-labeled glucose and acetate can produce distinct isotopomers of metabolites, which could be used to track multiple intermediate products of TCA cycle in the CNS. Therefore, specific ^{13}C-labeled glucose and acetate (or ethanol) combined with in vivo ^{13}C MRS can be used to observe brain metabolism and glutamatergic neurotransmission. In other words, co-administration of differently ^{13}C-labeled substrates combined with analysis of multiple ^{13}C MRS signals in the spectral region of carboxylic/amide carbons allows investigators to cleanly separate the contributions to Glu, Gln, and Asp from different energy substrates.

In the present study, when [1-^{13}C]ethanol and [$^{13}C_6$]-D-glucose were intravenously administrated to the animals, GluC5, GluC1, GlnC5, GlnC1, and AspC4, originated from both [$^{13}C_6$]-D-glucose and [1-^{13}C]ethanol could be detected over the 171–186 ppm range (Fig. 4), as could the fine isotopomer structure arising from homonuclear ^{13}C-^{13}C *J*-couplings. The isotopomer patterns observed in vivo are consistent with the known ^{13}C-^{13}C *J*-couplings previously detected in both in vitro and in vivo studies (19,35).

There was a striking similarity between the steady state spectra acquired using [$^{13}C_6$]-D-glucose and [1-^{13}C] ethanol with the corresponding results of the co-infusion of [$^{13}C_6$]-D-glucose and [1-^{13}C] acetate (52,53). Obviously, in both spectra, the singly labeled substrate (acetate or ethanol) makes a predominant contribution to glial glutamine. This similarity can be explained by the conversion of ethanol into acetate in the liver and the subsequent recirculation of acetate into the brain. In addition, the features of the spectra acquired during co-infusions match the sum of the corresponding single substrate ([$^{13}C_6$]-D-glucose, [1-^{13}C]ethanol and [1-^{13}C]acetate) infusion spectra (52,53). Thus, the present study demonstrate that the metabolic consequence of ethanol consumption can be detected in the brain by noninvasive ^{13}C MRS. The strong similarity of in vivo ^{13}C spectra acquired with ethanol administration to intravenous acetate infusion suggests that orally administered ethanol may be used as a glia-specific substrate to study cerebral metabolism.

Following the above reasoning, a mixture of [$^{13}C_6$]-D-glucose and [1-^{13}C]ethanol was intragastrically administered to the group D animals. Fig. 5 indicates that the results are similar to those experiments that used intravenous co-infusion of [$^{13}C_6$]-D-glucose and [1-^{13}C]ethanol, except that a temporal lag in the appearance of doublet peaks was observed in the intragastric administration experiments. This was due to the fact that it took more time for uniformly labeled glucose to reach blood circulation. Many early studies of acetate metabolism found that it was impossible to raise blood acetate levels by oral ingestion of acetic acid or acetate, however, when moderate amounts of ethanol were given, acetate concentrations increased several-fold over oral ingestion of acetate (47). Furthermore, for safety reasons, studies with ^{13}C-labeled chemicals in humans are generally conducted using lower doses of acetate infusion than in animal studies (20). The rate at which ethanol was cleared from the blood was the same as the rate of acetate production (47), suggesting that the enzymatic and chemical processes leading from ethanol to free acetate are quite powerful and rapid.

Chronic alcohol consumption is usually associated with metabolic disturbances of sulfur-containing amino acids, leading to increased levels of glutamate, aspartate, and homocysteine in alcoholic patients, and may result in dependence, addiction, and even liver cirrhosis. When high resolution proton NMR spectroscopy, which offers superior dynamic range and detects many classes of molecules in samples of brain tissue extracts or serum, was used to observe the effects of an acute or single administration of ethanol on metabolic alterations in the CNS, no detectable changes in the brain were observed (54). Even at pharmacologically relevant concentrations, and particularly in the concentration range of 10 to 20 mM, the effect of ethanol on the “fluidity” of the membrane bulk lipids is very small, or undetectable (1). In contrast, the results of the present study suggest that oral or intragastric administration of ^{13}C-labeled ethanol could be used to study brain metabolism and neurotransmission using ^{13}C MRS.

Acknowledgments

The authors are grateful to Dr. Su Xu, Mr. Christopher Johnson, and Dr. Steve Li for valuable help. Ms. Ioline Henter provided editorial assistance. This work was supported by the Intramural Research Program of the National Institute of Mental Health, National Institutes of Health, Department of Health and Human Services (IRP-NIMH-NIH-DHHS).

Abbreviations used

ADH	dehydrogenase
Cata	catalase
CYP2E1	cytochrome P450 2E1
BBB	blood-brain barrier
ALDH	Aldehyde dehydrogenase
MRS	magnetic resonance spectroscopy
TCA	tricarboxylic acid
GABA	γ-amminobutyric acid
CMT	^{13}C magnetization transfer
CNS	central nervous system
RF	radio frequency
RARE	rapid acquisition with relaxation enhancement
MRI	magnetic resonance imaging
NOE	nuclear Overhauser enhancement
CW	continuous-wave
AHP	adiabatic half passage
AcHC1	[1-^{13}C]acetaldehyde
GluC5	[5-^{13}C]glutamate
GlnC5	[5-^{13}C]glutamine
[1-^{13}C]γ-aminobutyric acid	GABAC1
[4-^{13}C]aspartate	AspC4
AspC1	[1-^{13}C]aspartate
BW	body weight
lb	line broadening
NAA	Nacetylaspartate
gb	Gaussian broadening
PET	positron emission tomography

References

1. Eckardt MJ, File SE, Gessa GL, Grant KA, Guerri C, Hoffman PL, Kalant H, Koob GF, Li TK, Tabakoff B. Effects of moderate alcohol consumption on the central nervous system. Alcohol Clin Exp Res. 1998; 22:998–1040. [PubMed: 9726269]
2. Mukherji B, Kashiki Y, Ohyanagi H, Sloviter HA. Metabolism of ethanol and acetaldehyde by the isolated perfused rat brain. J Neurochem. 1975; 24:841–843. [PubMed: 235601]
3. Deng XS, Deitrich RA. Putative role of brain acetaldehyde in ethanol addiction. Curr Drug Abuse Rev. 2008; 1:3–8. [PubMed: 19122804]
4. Lutwak-Mann C. Alcohol dehydrogenase of animal tissues. Biochem J. 1938; 32:1364–1374. [PubMed: 16746762]

5. Towne JC. Effect of ethanol and acetaldehyde on liver and brain monoamine oxidase. Nature. 1964; 201:709–710. [PubMed: 14134720]

6. Deitrich R, Zimatkin S, Pronko S. Oxidation of ethanol in the brain and its consequences. Alcohol Res Health. 2006; 29:266–273. [PubMed: 17718405]

7. Westcott JY, Weiner H, Shultz J, Myers RD. In vivo acetaldehyde in the brain of the rat treated with ethanol. Biochem Pharmacol. 1980; 29:411–417. [PubMed: 7362655]

8. Petersen DR. Aldehyde dehydrogenase and aldehyde reductase in isolated bovine brain microvessels. Alcohol. 1985; 2:79–83. [PubMed: 3893467]

9. Tampier L, Cariz S, Quintanilla ME. Metabolism of acetaldehyde by rat isolated aortic rings: does endothelial tissue contribute to its extrahepatic metabolism? Alcohol. 1993; 10:203–206. [PubMed: 8507388]

10. Tampier L, Quintanilla ME, Letelier C, Mardones J. Effect of 3-amino-1,2,4-triazole on narcosis time and lethality of ethanol in UChA rats. Alcohol. 1988; 5:5–8. [PubMed: 3355670]

11. Aragon CM, Rogan F, Amit Z. Ethanol metabolism in rat brain homogenates by a catalase-H2O2 system. Biochem Pharmacol. 1992; 44:93–98. [PubMed: 1632841]

12. Gill K, Menez JF, Lucas D, Deitrich RA. Enzymatic production of acetaldehyde from ethanol in rat brain tissue. Alcohol Clin Exp Res. 1992; 16:910–915. [PubMed: 1443429]

13. Zimatkin SM, Buben AL. Ethanol oxidation in the living brain. Alcohol alcohol. 2007; 42:529–532. [PubMed: 17660523]

14. Mushahwar IK, Koeppe RE. Incorporation of label from [1-^{14}C]ethanol into the glutamate-glutamine pools of rat brain in vivo. Biochem J. 1972; 126:467–469. [PubMed: 5075261]

15. Dimitrakopoulou-Strauss A, Strauss LG, Gutzler F, Irngartinger G, Kontaxakis G, Kim DK, Oberdorfer F, van Kaick G. Pharmacokinetic imaging of 11C ethanol with PET in eight patients with hepatocellular carcinomas who were scheduled for treatment with precutaneous ethanol injection. Radiology. 1999; 211:681–686. [PubMed: 10352591]

16. García-Espinosa MA, Rodrigues TB, Sierra A, Benito M, Fonseca C, Gray HL, Bartnik BL, García-Martín ML, Ballesteros P, Cerdán S. Cerebral glucose metabolism and the glutamine cycle as detected by in vivo and in vitro 13C NMR spectroscopy. Neurochem Int. 2004; 45:297–303. [PubMed: 15145545]

17. Yang J, Shen J. Elevated endogenous GABA concentration attenuates glutamate-glutamine cycling between neurons and astroglia. J Neural Transm. 2009; 116:291–300. [PubMed: 19184333]

18. Li S, Zhang Y, Wang S, Yang J, Ferraris Araneta M, Farris A, Johnson C, Fox S, Innis R, Shen J. In vivo 13C magnetic resonance spectroscopy of human brain on a clinical 3 T scanner using [2-13C]glucose infusion and low-power stochastic decoupling. Magn Reson Med. 2009; 62:565–573. [PubMed: 19526500]

19. Cerdan S, Künnecke B, Seelig J. Cerebral metabolism of [1,2-13C2]acetate as detected by in vivo and in vitro 13C NMR. J Biol Chem. 1990; 265:12916–12926. [PubMed: 1973931]

20. Shen J, Petersen KF, Behar KL, Brown P, Nixon TW, Mason GF, Petroff OA, Shulman GI, Shulman RG, Rothman DL. Determination of the rate of the glutamate/glutamine cycle in the human brain by in vivo 13C NMR. Proc Natl Acad Sci U S A. 1999; 96:8235–8240. [PubMed: 10393978]

21. Shulman, RG.; Rothman, DL. Brain energetics and neuronal activity. Chichester, UK: John Wiley & Sons; 2004.

22. Taylor A, McLean M, Morris P, Bachelard H. Approaches to studies on neuronal/glial relationships by 13C-MRS analysis. Dev Neurosci. 1996; 18:434–442. [PubMed: 8940616]

23. Morris P, Bachelard H. Reflections on the application of 13C-MRS to research on brain metabolism. NMR Biomed. 2003; 16:303–312. [PubMed: 14679497]

24. Hassel B, Sonnewald U, Fonnum F. Glial-neuronal interactions as studied by cerebral metabolism of [2–13C] acetate and [1–13C]glucose: an ex vivo 13C NMR spectroscopic study. J Neurochem. 1995; 64:2773–2782. [PubMed: 7760058]

25. Lebon V, Petersen KF, Cline GW, Shen J, Mason GF, Dufour S, Behar KL, Shulman GI, Rothman DL. Astroglial contribution to brain energy metabolism in humans revealed by 13C nuclear magnetic resonance spectroscopy: elucidation of the dominant pathway for neurotransmitter

glutamate repletion and measurement of astrocytic oxidative metabolism. J Neurosci. 2002; 22:1523–1531. [PubMed: 11880482]

26. Shic F, Ross B. Automated data processing of [1H-decoupled] 13C MR spectra acquired from human brain in vivo. J Magn Reson. 2003; 162:259–268. [PubMed: 12810010]
27. Yang J, Li SS, Bacher J, Shen J. Quantification of cortical GABA-glutamine cycling rate using in vivo magnetic resonance signal of [2–13C]GABA derived from glia-specific substrate [2–13C]acetate. Neurochem Int. 2007; 50:371–378. [PubMed: 17056156]
28. Li S, Chen Z, Zhang Y, Lizak M, Bacher J, Innis RB, Shen J. In vivo single-shot, proton-localized 13C MRS of rhesus monkey brain. NMR Biomed. 2005; 18:560–569. [PubMed: 16273509]
29. Mayfield ED, Bensadoun A, Johnson BC. Acetate metabolism in ruminant tissues. J Nutr. 1966; 89:189–196. [PubMed: 5944095]
30. Mendelson JH, Woods BT, Chiu TM, Mello NK, Lukas SE, Teoh SK, Sintavanarong P, Cochin J, Hopkins MA, Dobrosielski M. In vivo proton magnetic resonance spectroscopy of alcohol in human brain. Alcohol. 1990; 7:443–447. [PubMed: 2222847]
31. Xu S, Yang J, Shen J. In vivo 13C saturation transfer effect of the lactate dehydrogenase reaction. Magn Reson Med. 2007; 57:258–264. [PubMed: 17260357]
32. Yang J, Singh S, Shen J. 13C saturation transfer effect of carbon dioxide-bicarbonate exchange catalyzed by carbonic anhydrase in vivo. Magn Reson Med. 2008; 59:492–498. [PubMed: 18224701]
33. Yang J, Xu S, Shen J. Fast isotopic exchange between mitochondria and cytosol in brain revealed by relayed 13C magnetization transfer spectroscopy. J Cereb Blood Flow Metab. 2009; 29:661–669. [PubMed: 19156161]
34. Li S, Shen J. Integrated RF probe for in vivo multinuclear spectroscopy and functional imaging of rat brain using an 11.7 Tesla 89 mm bore vertical microimager. MAGMA. 2005; 18:119–127. [PubMed: 16007474]
35. Xu S, Shen J. In vivo dynamic turnover of cerebral 13C isotopomers from [U-13C]glucose. J Magn Reson. 2006; 182:221–228. [PubMed: 16859940]
36. Chen Z, Li SS, Yang J, Letizia D, Shen J. Measurement and automatic correction of high-order B0 inhomogeneity in the rat brain at 11.7 Tesla. Magn Reson Imaging. 2004; 22:835–842. [PubMed: 15234452]
37. Irving MG, Simpson SJ, Brooks WM, Holmes RS, Doddrell DM. Application of the reverse DEPT polarization-transfer pulse sequence to monitor in vitro and in vivo metabolism of 13C-ethanol by 1H-NMR spectroscopy. Int J Biochem. 1985; 17:471–478. [PubMed: 3159605]
38. Brooks WM, Moxon LN, Field J, Irving MG, Doddrell DM. In vitro metabolism of [2-13C]-ethanol by 1H NMR spectroscopy using 13C decoupling with the reverse DEPT polarization-transfer pulse sequence. Biochem Biophys Res Commun. 1985; 128:107–112. [PubMed: 3157376]
39. San George RC, Hoberman HD. Reaction of acetaldehyde with hemoglobin. J Biol Chem. 1986; 261:6811–6821. [PubMed: 3700416]
40. Sheridan RP, Deakyne CA, Allen LC. Acetaldehyde hydrate and carbonic anhydrase: possible roles in the inhibition of brain aldehyde dehydrogenase. Adv Exp Med Biol. 1980; 132:705–713. [PubMed: 6775515]
41. Li S, Yang J, Shen J. Novel strategy for cerebral 13C MRS using very low RF power for proton decoupling. Magn Reson Med. 2007; 57:265–271. [PubMed: 17260369]
42. Yang J, Johnson C, Shen J. Detection of reduced GABA synthesis following inhibition of GABA transaminase using in vivo magnetic resonance signal of [13C]GABA C1. J Neurosci Methods. 2009; 182:236–243. [PubMed: 19540876]
43. Mason GF, Falk Petersen K, de Graaf RA, Kanamatsu T, Otsuki T, Shulman GI, Rothman DL. A comparison of (13)C NMR measurements of the rates of glutamine synthesis and the tricarboxylic acid cycle during oral and intravenous administration of [1– (13)C]glucose. Brain Res Brain Res Protoc. 2003; 10:181–190. [PubMed: 12565689]
44. Selmer J, Grunnet N. Ethanol metabolism and lipid synthesis by isolated liver cells from fed rats. Biochem Biophys Acta. 1976; 428:123–137. [PubMed: 1260014]
45. Kilanmaa K, Virtanen P. Ethanol and acetaldehyde levels in cerebrospinal fluid during ethanol oxidation in the rat. Neurosci Lett. 1978; 10:181–186. [PubMed: 19605277]

46. Jamal M, Ameno K, Uekita I, Kumihashi M, Wang W, Ijiri I. Catalase mediates acetaldehyde formation in the striatum of free-moving rats. Neurotoxicology. 2007; 28:1245–1248. [PubMed: 17597213]
47. Lundquist F. Production and utilization of free acetate in man. Nature. 1962; 4815:579–580. [PubMed: 14467396]
48. Lundquist F, Tygstrup N, Winkler K, Mellemgaard K, Munck-petersen S. Ethanol metabolism and production of free acetate in the human liver. J Clin Invest. 1962; 41:955–961. [PubMed: 14467395]
49. Crabb DW, Bosron WF, Li TK. Ethanol metabolism. Pharmac Ther. 1987; 34:59–73.
50. Xu S, Shen J. Studying enzymes by in vivo C magnetic resonance spectroscopy. Prog Nucl Magn Reson Spectrosc. 2009; 55:266–283. [PubMed: 20161496]
51. Bachelard H. Landmarks in the application of 13C-magnetic resonance spectroscopy to studies of neuronal/glial relationships. Dev Neurosci. 1998; 20:277–288. [PubMed: 9778563]
52. Xiang, Y.; Shen, J. Alcohol as a substrate for acetate in ^{13}C MRS study of brain metabolism. ISMRM-ESMRMB 2010 Joint Annual Conference. MRS of animal brain; Stockholm, Sweden. 2010. p. 2384
53. Xiang, Y.; Shen, J. Simultaneous detection of metabolism of different substrates in the carboxylic/amide region using in vivo ^{13}C MRS at 11.7 Tesla. ISMRM-ESMRMB Joint Annual Conference. MRS of animal brain; Stockholm, Sweden. 2010. p. 2383
54. Nicholas PC, Kim D, Crews FT, Macdonald JM. 1H NMR-based metabolic analysis of liver, serum, and brain following ethanol administration in rats. Chem Res Toxicol. 2008; 21:408–420. [PubMed: 18095657]

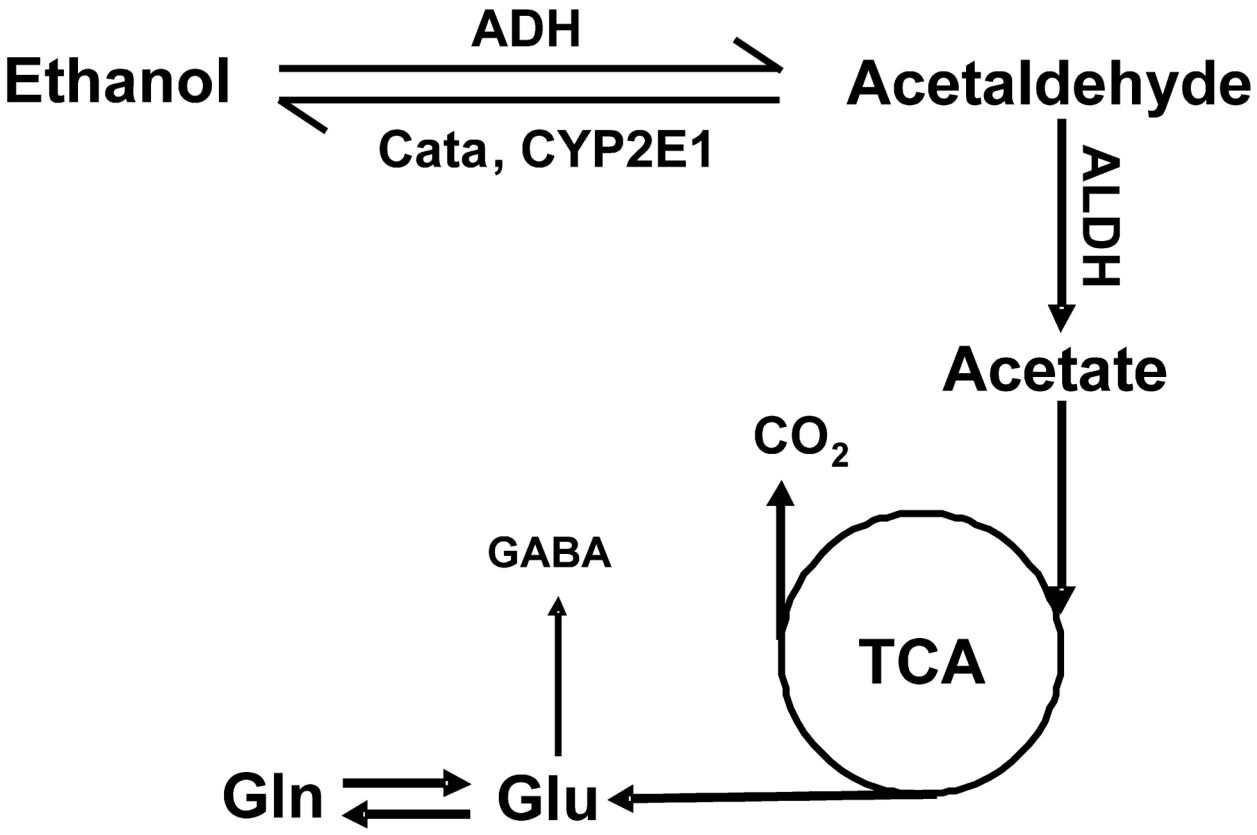

Figure 1.
Oxidative pathway of ethanol metabolism. Alcohol dehydrogenase (ADH), cytochrome P450E1 (CYP2E1), and catalase (Cata) are responsible for breaking down ethanol to acetaldehyde. Aldehyde dehydrogenase (ALDH) further converts acetaldehyde to acetate. Acetate from bloodstream enters the brain and is metabolized therein.

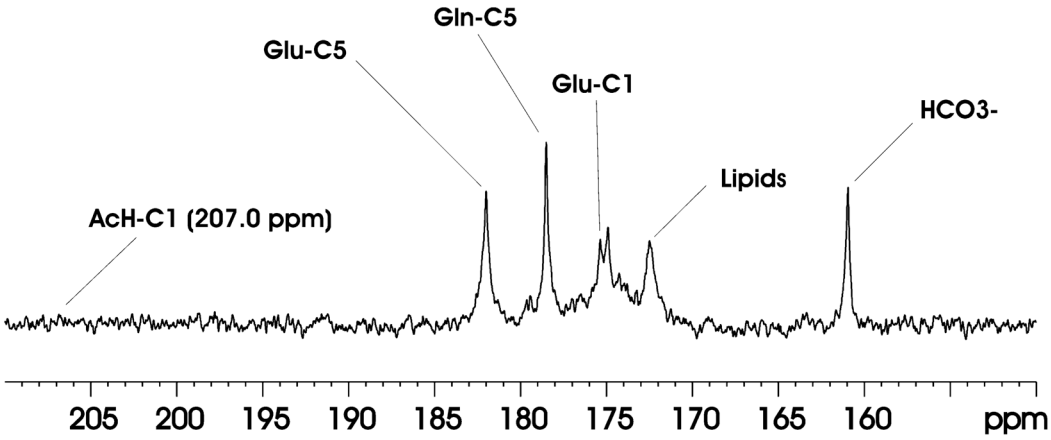

Figure 2.

Accumulated *in vivo* ^{13}C MRS spectrum (150~210 ppm) from the rat brain after 280 minutes intravenous infusion of [1-^{13}C]ethanol. TR = 18.75s, NA = 448. The spectrum was summed from one rat in Group A over 280 minutes. Data processing: lb = 10, si = 16k. Glu-C5 = glutamate C5, Gln-C5 = glutamine C5, Glu-C1 = glutamate C1, Gln-C1 = glutamine C1, AcH-C1 = acetaldehyde C1.

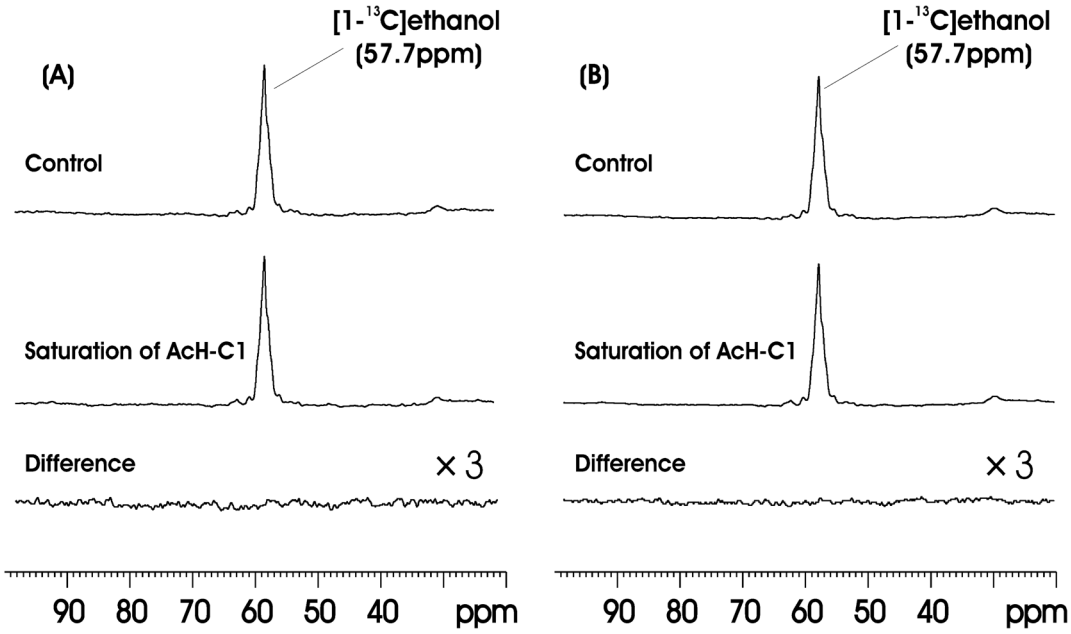

Figure 3.

(A) Results of the ^{13}C saturation transfer experiments on one Group B animal targeting the [1-^{13}C]ethanol↔[1-^{13}C]acetaldehyde reaction. Top trace: control spectrum; middle trace: with saturation of AcH-C1 at 207.00ppm; bottom trace: difference spectrum (×3). The difference spectrum (right bottom trace) represents signal averaged for 180 min (TR = 9.375s, NA = 1152, lb = 10). (B) Summed spectra from 5 Group B rats. The difference spectrum (bottom right trace) represents signal averaged for 900 min (TR = 9.375s, NA = 5760, lb = 10).

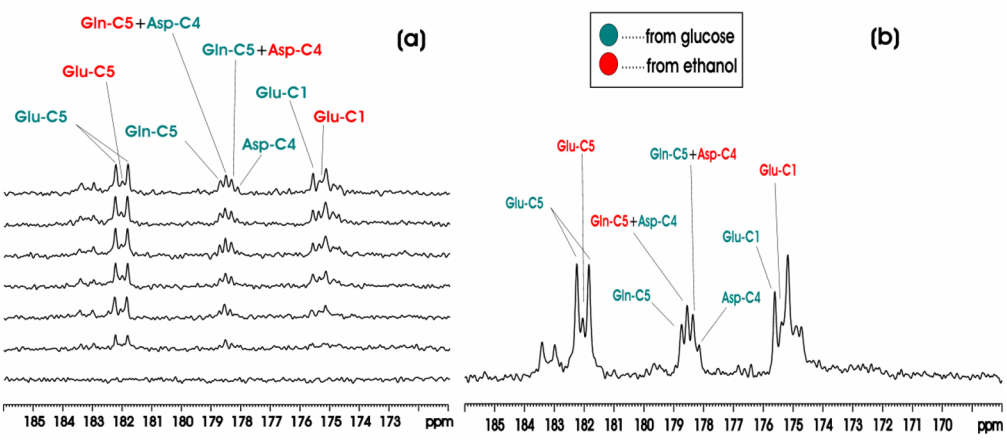

Figure 4.

(a) Time-course *in vivo* ^{13}C MRS spectra from an individual rat brain during co-infusion of [1-^{13}C]ethanol and [$^{13}C_6$]-D-glucose compared with baseline (bottom trace). Each individual spectrum was averaged for 20 minutes with NA = 32. (b) *In vivo* ^{13}C MRS spectrum from an individual rat brain accumulated during the 120–360 minute interval after the start of co-infusion of [1-^{13}C]ethanol and [$^{13}C_6$]-D-glucose. Green: resonance lines originated from [$^{13}C_6$]-D-glucose; Red: resonance lines originated from [1-^{13}C]ethanol. lb= -5, gb = 0.1. Note the glutamate C5 resonance labeled by [$^{13}C_6$]-D-glucose formed a doublet with a ^{13}C-^{13}C homonuclear J coupling constant of 51 Hz; the glutamate C5 resonance labeled by [1-^{13}C]ethanol formed a singlet. From downfield to upfield, the resonance lines in the 178–179 ppm region were Gln C5 by [$^{13}C_6$]-D-glucose, Gln C5 by [1-^{13}C]ethanol + Asp C4 by [$^{13}C_6$]-D-glucose, Gln C5 by [$^{13}C_6$]-D-glucose + Asp C4 by [1-^{13}C]ethanol, Asp C4 by [$^{13}C_6$]-D-glucose. The two downfield Glu C1 lines originated from [$^{13}C_6$]-D-glucose and [1-^{13}C]ethanol were also marked.

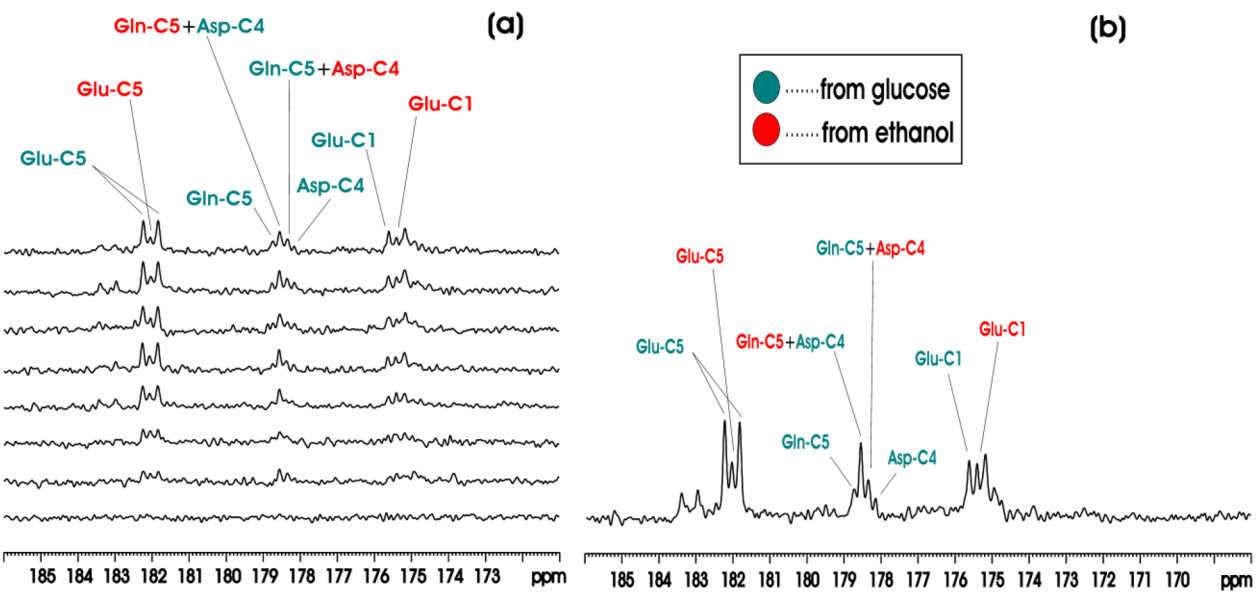

Figure 5.

(a) Time-course ^{13}C MRS spectra from an individual rat brain during intragastric co-administration of [1-^{13}C]ethanol and [$^{13}C_6$]-D-glucose. Each individual spectrum was averaged for 20 minutes. The bottom spectrum was the baseline. (b) Accumulated *in vivo* ^{13}C MRS spectra from an individual rat brain during intragastric co-administration of [1-^{13}C] ethanol and [$^{13}C_6$]-D-glucose. The spectrum was summed during the 140~360 minute interval after the start of the co-infusion. Green: resonance lines originated from [$^{13}C_6$]-D-glucose; Red: resonance lines originated from [1-^{13}C]ethanol. Data processing parameters were: lb = −5, gb = 0.1.